Hydrophobic Pockets at the Membrane Interface: An Original Mechanism for Membrane Protein Interactions†

Véronique Arluison,*,‡ Jérôme Seguin,‡ Jean-Pierre Le Caer,§ James N. Sturgis,‡,||,⊥ and Bruno Robert‡,⊥

Service de Biophysique des Fonctions Membranaires, DBJC/CEA and URA 2096 CNRS, CE Saclay, 91191 Gif/Yvette Cedex, France, and ESPCI, CNRS UMR 7637, 10 rue Vauquelin, 75005 Paris, France

Received September 16, 2003; Revised Manuscript Received November 19, 2003

ABSTRACT: The effect of partial digestion by trypsin and GluC protease on the association of the membrane polypeptides of LH1 from *Rhodospirillum* (*Rsp.*) *rubrum* was studied. Trypsin and GluC protease treatments of LH1 result in the cleavage of the first three amino acids from the α polypeptide and of the first 18 amino acids from the *β* polypeptide, respectively, without any noticeable reorganization of their secondary structure, as measured by attenuated total reflectance Fourier transform IR spectroscopy. However, the enthalpy variation accompanying dimer formation was dramatically reduced by the protease attacks by as much as 80%. Our results show that the α*β* heterodimer is mainly stabilized by hydrophobic interactions which involve the amino-terminal extensions of the participating polypeptides. Using the close homology between the polypeptides of *Rsp. rubrum* LH1 and that of *Rsp. molischianum* LH2, whose structure is known, a structural model for these "hydrophobic pockets" lying close to the membrane interface is proposed.

α-Helical integral membrane proteins play a key role in signal transduction and molecule transport in the cell. They are organized around the association of two or more transmembrane α-helices, which often bind ligands and/or cofactors. Although they play a role in many essential biological processes, little is still known about the factors and forces that drive their association. Interaction motifs, found at helix−helix interfaces as well as interhelical H-bonding, have been suggested to play an important role in helix−helix association within the hydrophobic membrane region (see, e.g., refs *1*−*3*). From the point of view of helix−helix association, one of the best characterized membrane proteins is the core antenna protein LH1 from the *Rhodospirillum* (*Rsp.*) *rubrum* purple bacteria. This protein ensures the capture of the solar photons and the efficient funneling of the resulting excitation energy toward the photochemical reaction center (RC).[1] It is composed of two small (ca. 50 amino acids) integral membrane polypeptides, namely, α and *β* (Figure 1). In the fully assembled protein, α*β* heterodimers associate to form circular oligomers of 16 α*β* subunits (*4*). Similar structures have been obtained from two-dimensional crystals of core antenna of different species of purple bacteria (*5*−*8*). Each of these polypeptides binds a bacteriochlorophyll (BChl) molecule via an histidyl residue located in the transmembrane domain. These BChl molecules form a circular array of excitonically interacting molecules in the fully assembled protein.

The electronic properties of LH1 thus intimately depend on the association state of the polypeptides of which they are composed (see, e.g., refs *9*−*12*). Fully assembled LH1 proteins from the carotenoidless strain of *Rsp. rubrum* G9+ absorb at 873 nm. Once purified, they can be reversibly dissociated in the presence of the detergent *n*-octyl *β*-D-glucopyranoside (*β*OG) by a two-step mechanism. Addition of *β*OG first leads to a 820 nm absorbing form, which is mainly constituted by isolated α*β* heterodimers (*11*, *13*−*16*). Further increasing the *β*OG concentration causes the B820 dimeric form to dissociate into a 777 nm absorbing form (*17*, *18*). This latter form corresponds to monomeric α and *β* polypeptides still binding BChl (*13*). This stepwise dissociation process is completely reversible (*18*). Because of the possibility of following the dissociation process by absorption spectroscopy, the LH1 protein is an ideal model for the study of α-helical interactions in membrane proteins. The possibility of reversibly dissociating the LH1 was used to estimate the thermodynamic parameters associated with the B820 formation (*13*) or the full association of LH1 (B873) by varying the temperature or detergent concentration (*14*). By making use of modified LH1 polypeptides, we have determined some of the structural elements required for their association (*19*, *20*). In this paper, we have studied how the thermodynamic parameters of the B777/B820 association reaction are modified by the cleavage of the short soluble extensions of the α and *β* polypeptides using trypsin and

† This work was supported by CEA and CNRS. V.A. was supported by a postdoctoral fellowship from the CEA.

* Address correspondence to this author at IBPC, 13 rue P. et M. Curie, 75005 Paris, France. E-mail: Veronique.Arluison@ibpc.fr. Phone: 33-1 58 41 51 39. Fax: 33-1 58 41 50 20.

‡ Service de Biophysique des Fonctions Membranaires.

§ ESPCI.

|| Present address: LISM/IBSM, CNRS, 31 ch. J. Aiguier, 13402 Marseille Cedex 20, France.

⊥ These authors contributed equally to this work.

[1] Abbreviations: ATR-FTIR, attenuated total reflectance Fourier transform infrared; Bchl, bacteriochlorophyll; B873, B820, and B777, dissociated forms of light harvesting complex 1 absorbing at 873, 820, and 777 nm, respectively; CMC, critical micellar concentration; LH, light harvesting complex; K_d, equilibrium dissociation constant; MALDI-TOF, matrix-assisted laser desorption ionization mass spectrometry−time of flight; *β*OG, *n*-octyl *β*-D-glucopyranoside; RC, reaction center; *Rsp.*, *Rhodospirillum*; SDS−PAGE, sodium dodecyl sulfate−polyacrylamide gel.

10.1021/bi030205v CCC: $27.50
Published on Web 01/10/2004

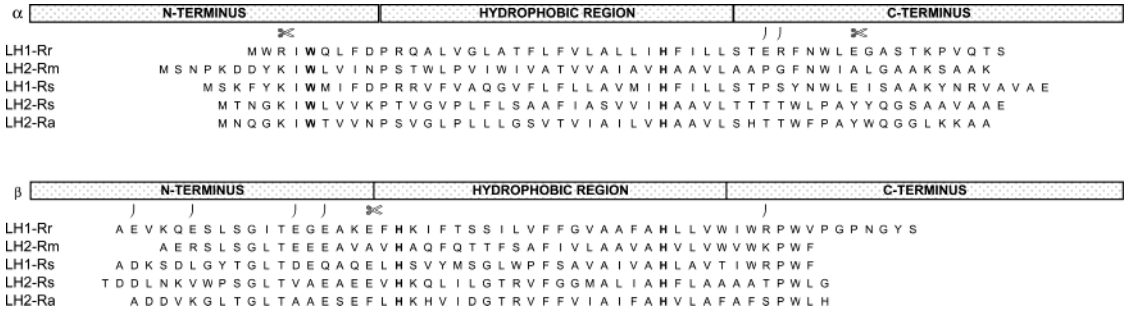

FIGURE 1: Primary sequence of the α and *β* polypeptides of different bacterial LH (*36*, *37*): Rr, *Rsp. rubrum*; Rm, *Rsp. molischianum*; Rs, *Rb. sphaeroides*; Ra, *Rhodopseudomonas acidophila*. Key:), potential cleavage sites; scissors, sites of protease cleavage.

GluC protease, respectively. We find that the B820 α*β* dimer is stabilized by interactions of hydrophobic nature which occur essentially close to the membrane interface, at the amino-terminal end of these polypeptides. Using the homology between the polypeptides of *Rsp. rubrum* LH1 and of *Rhodospirillum molischianum* LH2, the structure of which is known (*21*), the nature of these "hydrophobic pockets", present at the membrane interface and which play a key role in the B820 stabilization, is described.

MATERIALS AND METHODS

n-Octyl *β*-D-glucopyranoside was from Biomol (Germany), and trypsin, GluC, and α_2-macroglobulin were from Roche (Switzerland). Except as otherwise stated, all other chemicals were from Sigma Chemical Co. (St. Louis, MO) or Merck-Biochemicals (Germany).

Rsp. rubrum B820 was purified from the carotenoidless stain G9+ (*22*). The purification procedure was described earlier (*13*). After solubilization of the chromatophores with 2% *β*OG, LH1−RC are first purified on a DEAE-Sepharose ion-exchange chromatography column. B820 complexes are prepared by titration of LH1−RC complexes with 2% *β*OG and further purified using an anion-exchange column (FPLC Resource Q). The quality of the fractions collected was controlled by SDS−PAGE, followed by Coomassie staining. The whole purification procedure was performed in dim light at 4 °C. Protein concentrations were determined either from the absorption at 280 nm (absorption coefficient at 280 nm calculated from the amino acid composition, $\epsilon_{280}^{1\text{mg/mL}} = 2.9$) or from the absorption at 777 or 820 nm [absorption coefficients $\epsilon_{777} = 55\ \text{mM}^{-1}\ \text{cm}^{-1}$ and $\epsilon_{820} = 86\ \text{mM}^{-1}\ \text{cm}^{-1}$ (*23*)].

Trypsin and GluC digestions were performed in Tris-HCl, pH 8, containing 100 mM NaCl and 2% *β*OG, using 16.5 *μ*g of polypeptide concentration. Trypsin (500 ng) (diluted in 1 M $CaCl_2$ and 1 mM HCl) or GluC (1 *μ*g) was added per milligrams of B820. B820 was thus in large excess relative to both proteases. The reaction was followed by recording the absorption spectra between 700 and 900 nm of aliquots withdrawn from the solution. The reaction was stopped by adding the universal protease inhibitor α_2-macroglobulin (in a 1:1 ratio with endoproteinase).

Absorption spectra of the B820/B777 equilibrium were recorded at 20 °C with a Cary 5 spectrophotometer (Varian plc, Sidney). Absorption of the B777 and B820 forms was extracted from these spectra by decomposition using the GRAMS 32 software (Galactic, Salem, NH).

Mass spectra were recorded in positive reflectron mode with a Voyager STR-DE (Perseptive Biosystems, Framingham, MA) MALDI-TOF mass spectrometer equipped with a delayed extraction device. Samples were analyzed with the dried droplet method using a saturated solution of dihydroxybenzoic acid. Calibration was performed using insulin as a standard. For both proteases, digested polypeptides (approximately 0.5 mg/mL) were diluted (1/50 in 1% formic acid) and analyzed directly. Due to their poor solubility in water, the samples were not desalted using Zip Tips (Millipore).

Absorption spectra of the B820/B777 equilibrium were recorded in 20 mM Tris-HCl, pH 8, at various temperatures between 12 and 32 °C. Temperature measurements were made directly in the quartz cell. The apparent equilibrium constant, K_d, was derived from these absorption spectra, and the extinction coefficients of B820 and B777 using the equation:

$$\alpha + \beta \leftrightarrow \alpha\beta \qquad K_d = [820]/([777]/2)^2$$

The concentrations of both monomer [777] and dimer [820] were determined by spectral decomposition using the extinction coefficients of each of these species (*23*). From the variations of K_d with temperature, $\Delta H°$ and $\Delta S°$ of B820 dissociation could be determined.

Attenuated total reflectance FTIR spectra were measured with a Bruker vector 22 spectrophotometer equipped with a 45° diamond ATR attachment (National Instruments, U.K.). The spectra shown are the average of 125 scans after removal of the buffer signal.

Structural modeling of *Rsp. rubrum* B820 was performed using the *Rsp. molischianum* LH2 structure as a matrix (PDB entry 1LGH; *21*); the α and *β* polypeptides of the *Rsp. molischianum* LH2 share close sequence homology with those of *Rsp. rubrum* (26% and 52% sequence identity, respectively). The Swiss-Model server (*24*) was used to generate the structure of LH1 in dimeric form. The Bchl were positioned using the 1LGH structure. The dimer and the complex were energy minimized in 100 steps with a dielectric constant of 1 using the program CNS (*25*). The B820 structure is little different from the *Rsp. molischianum* structure (rms deviation of 0.48 Å for the 94 Cα atoms) and was deposited on PDB with the PDB entry 1NWO. Twelve amino acids from the α polypeptide from *Rsp. rubrum* were however not included in this model, as they have no equivalent in *Rsp. molischianum*.

RESULTS

Limited Proteolysis of B820. Limited proteolysis of the B820 complex was performed by adding either trypsin or

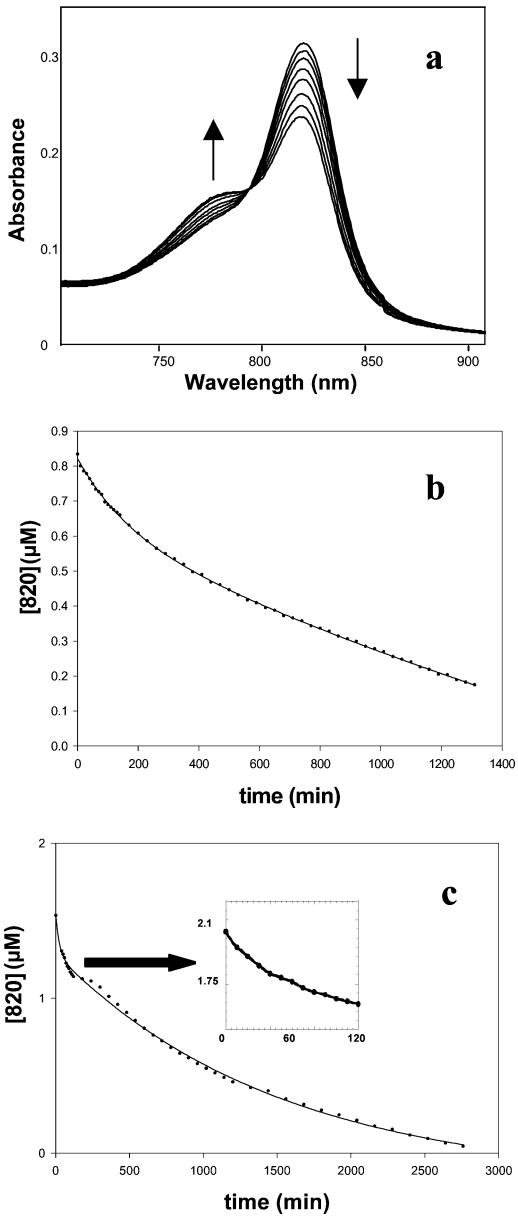

FIGURE 2: Limited proteolysis of B820. (a) Evolution of the electronic absorption spectrum of the B820/B777 equilibrium during digestion with trypsin. (b) Kinetics of B820 digestion by trypsin: solid line, single exponential fit of the experimental data ($k = 0.0013$ min^{-1}). (c) Kinetics for B820 digestion by GluC: solid line, double exponential fit of the experimental data ($k_1 = 0.041$ min^{-1}; $k_2 = 0.0007$ min^{-1}).

GluC proteases to an equilibrium B820/B777 mixture (initial conditions [820] = 20[777]). Digestion reactions could be followed by electronic absorption spectroscopy, as they led to the progressive dissociation of B820 dimers into B777 monomers (Figure 2). In the case of trypsin, the kinetics is monoexponential ($t_{1/2} = 500$ min). For GluC the protease attack exhibits two phases, a fast one ($t_{1/2} = 17$ min) and a much slower one ($t_{1/2} = 1000$ min). The reaction products were analyzed by electrophoresis (Figure 3). During trypsin proteolysis, no band corresponding to smaller polypeptides appears in the gel. In the presence of GluC, the β polypeptide is completely digested in 1 h into a fragment of approximately 4 kDa. The α polypeptide is digested much more slowly into a fragment of approximately 5 kDa. The fast phase observed in the presence of GluC can thus be assigned

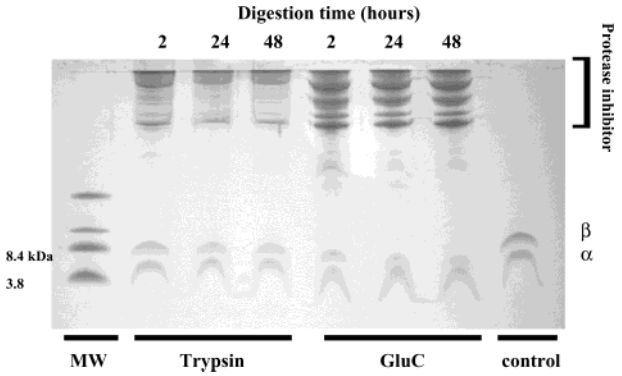

FIGURE 3: Effect of proteolysis on B820 polypeptides analyzed by SDS−PAGE. During GluC digestion, the β polypeptide is digested in 1 h into a fragment of approximately 4 kDa. The α polypeptide is digested more slowly into a fragment of approximately 5 kDa.

to β polypeptide digestion while the slow one corresponds to the attack of the α polypeptide.

The position(s) of the cleavage site(s) for each protease was (were) identified by MALDI-TOF mass spectrometry after a complete digestion. Trypsin treatment results in fragments of 6120 and 6177 for the α and β polypeptides, respectively. The β polypeptide is thus not cleaved by trypsin, and there is a single cleavage site on the α polypeptide, at the level of $R_{\alpha 3}$. GluC treatment results in fragments of 5116 and 4260 for the α and β polypeptides, respectively. The β polypeptide is cleaved by GluC at the level of $E_{\beta 18}$, and this must correspond to the fast phase in Figure 2. Cleavage of the α polypeptide occurs at the level of $E_{\alpha 42}$, with slower kinetics, as detected by MALDI-TOF. These results are in good agreement with the electrophoresis experiments (Figure 3). There are a number of potential cleavage sites on the LH polypeptides (see Figure 1). Although we cannot discard the possibility that GluC rapidly attacks the β polypeptide at positions 2, 6, 13, and 15, as such cleavages would not be detectable in the MALDI-TOF experiments, we may conclude that the $E_{\alpha 36}$, $R_{\alpha 37}$, and $R_{\beta 45}$ sites are protected from the protease digestion.

When partial digestion by trypsin is performed on the fully associated LH1 protein, attack of the N-terminal end of the α polypeptide is considerably slowed ($t_{1/2} = 5000$ min; results not shown). This suggests that the $R_{\alpha 3}$ cleavage site is protected against trypsin in the intact complex. Overnight dialysis at 4 °C of the trypsin-digested B820 against buffer without βOG induces a red shift of the main absorption Q_y transition of this complex to 869 nm (data not shown). The precise position of this transition is not identical to that of intact LH1 (873 nm), but the observation of a similar Q_y position has been reported when quickly diluting the B820 in the absence of detergent (*11*). As it is known that $(\alpha\beta)_2$ tetramers absorb at ca. 852 nm (*26*), such a 869 nm form should correspond to higher order oligomers. The cleavage of the first amino acids of the α polypeptide does thus not impair the ability of the $\alpha\beta$ dimer to further associate, suggesting that they are not playing a crucial role in $\alpha\beta$ dimer/dimer association.

Effect of Digestion on the B820 Structure. Protease treatments, although they induce dissociation of the B820 into B777, have, in most cases, no effect on the individual electronic absorption spectra of these two forms. Only after

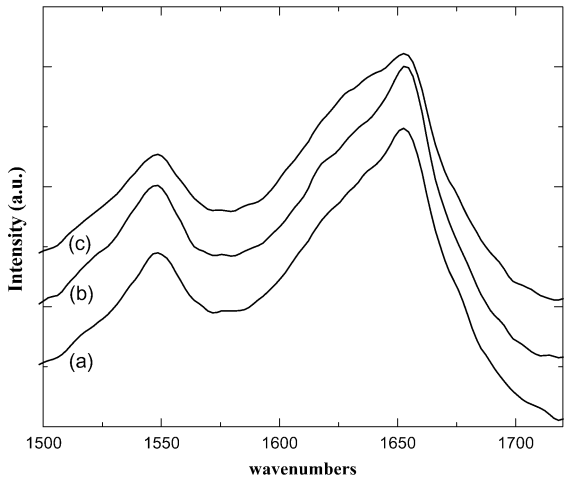

FIGURE 4: ATR-FTIR spectra (1500−1720 cm^{-1} region) of B820 complexes: (a) untreated; (b) after trypsin treatment; (c) after GluC treatment.

complete digestion of α and β by GluC (48 h digestion; results not shown) is the position of the B820 electronic transition shifted toward the blue, by 3 nm. The cleavage site of GluC in the α polypeptide is located two residues away from the $W_{\alpha 40}$, which forms an H-bond with the α-bound BChl molecule (*27*, *28*). This change in electronic properties of the B820 may reflect a change in the electrostatic environment of the interacting Bchl molecules, such as a partial exposure of the BChl binding site. Alternatively, the proteolysis might cause a partial destabilization of the BChl/BChl pair and of the associated polypeptide structure. As these effects are likely to interfere with the stability of the complex, in the following we have focused our studies on B820 exposed for 1 h only to GluC, i.e., after a period of time leading essentially to the digestion of the β polypeptide (see above).

The structural impact of the polypeptide cleavage by the proteases on the protein secondary structure was evaluated by infrared absorption spectroscopy. Figure 4 displays the higher frequency region of the FTIR spectra of native and digested B820. This spectral region contains the amide I band, which is particularly sensitive to the secondary structure of proteins. The main peak of the amide I band is observed for the three proteins at 1650 cm^{-1}, a position typical for α-helix-containing peptides. Trypsin digestion induces only a very slight difference on these spectra. After normalization of the spectra according to the number of amino acids present in each sample (i.e., 106 for the intact sample and 103 for the trypsin-digested one), it may be concluded that trypsin digestion results in a slight decrease in the intensity of the 1633 cm^{-1} shoulder of the main 1650 cm^{-1} band. Cleavage at $R_{\alpha 3}$ does thus not perturb the α-helical content of the B820 polypeptides. In the spectra of GluC-treated B820, the contribution at 1650 cm^{-1} also becomes higher as compared to the shoulder at 1630 cm^{-1}. Taking into account that 18 amino acids have been removed from the β polypeptide, about 30% (i.e., about 6) of the missing amino acids were in α-helical conformation before the GluC treatment, the remaining 12 being either in the extended or in the random coil conformation.

Thermodynamics of B777 Association into B820. The dissociation of dimeric B820 into momeric B777 is strongly temperature dependent. Increasing temperature favors dissociation of B820 into B777; this property has been used to determine the thermodynamic parameters of the association of the $\alpha\beta$ polypeptides (*13*−*16*, *29*). Protease-induced cleavage of these polypeptides at constant temperature favors dissociation of B820 into B777 (Figure 2), suggesting a partial destabilization of the dimers. To determine quantitatively the role of the cleaved extensions, the temperature dependence of the B820/B777 equilibrium was measured after trypsin and/or GluC digestion (reaction times of 10 and 1 h, respectively). For each sample, the concentrations of both monomer [777] and dimer [820] were determined by spectral decomposition at various temperatures using the extinction coefficients of each of these species (*23*). From these concentrations, the equilibrium constant was calculated, and from the temperature dependence of this, the thermodynamic parameters $\Delta H°$ and $\Delta S°$ for the dissociation of B820 dimers into B777 monomers were calculated (Figure 5). The values calculated for $\Delta H°$ are −99 and −28 kJ mol^{-1} for trypsin- and GluC-treated B820, respectively; the corresponding values for ΔS^0 are −0.22 and −0.12 kJ mol^{-1} K^{-1}. If the GluC reaction is performed until the carboxy-terminal part of the α polypeptide is digested, the B820 form completely disappears, indicating a dramatic destabilization of the $\alpha\beta$ dimer.

After 48 h at 30 °C in the absence of protease, we observed a decrease of the $\Delta H°$ associated with the dissociation of the control sample, from −180 to −140 kJ mol^{-1}. It could be due to the appearance in the sample of polypeptides unable to associate normally, for example, due to prolyl−peptide bond isomerization. The variations in the thermodynamic parameters are thus much larger in the protease-attacked samples than in the control one, although the latter was incubated for a much longer time at 30 °C (48 h vs 1 and 12 h for GluC and trypsin, respectively). This indicates that the enthalpy variations observed are mainly due to the modifications of the polypeptides by the protease and not to indirect, nonspecific effects induced by the incubation at 30 °C itself.

Role of the Ionic Strength in B820 Stabilization. These results suggest an important role for the soluble extensions of the α and β polypeptide in the B820 stabilization. To check the nature of the interactions involved at the level of these extensions, the B820/B777 equilibrium was exposed to increasing ionic strengths, and the amount of each species was calculated from the evolution of the absorption spectra. Increasing the ionic strength at constant temperature favors the B820 associated form (from 10 to 14 μM between 0 and 3 M NaCl; data not shown). It is known that the CMC of βOG is sensitive to the ionic strength, decreasing from 25 mM in the absence of salt to 12 mM at 1 M ionic strength in pure water (*30*). Such a decrease of the CMC, resulting in the increase of volume of the accessible hydrophobic phase at high salt concentration, should favor the dissociation of the B820 form into B777. The slight increase of B820 in the equilibrium thus clearly indicates that the $\alpha\beta$ association is favored when increasing the ionic strength, although variations of the CMC of the detergent do not allow a precise quantification.

DISCUSSION

In this paper, the effect of limited proteolysis on B820 structure and stability was analyzed quantitatively. Cleavage

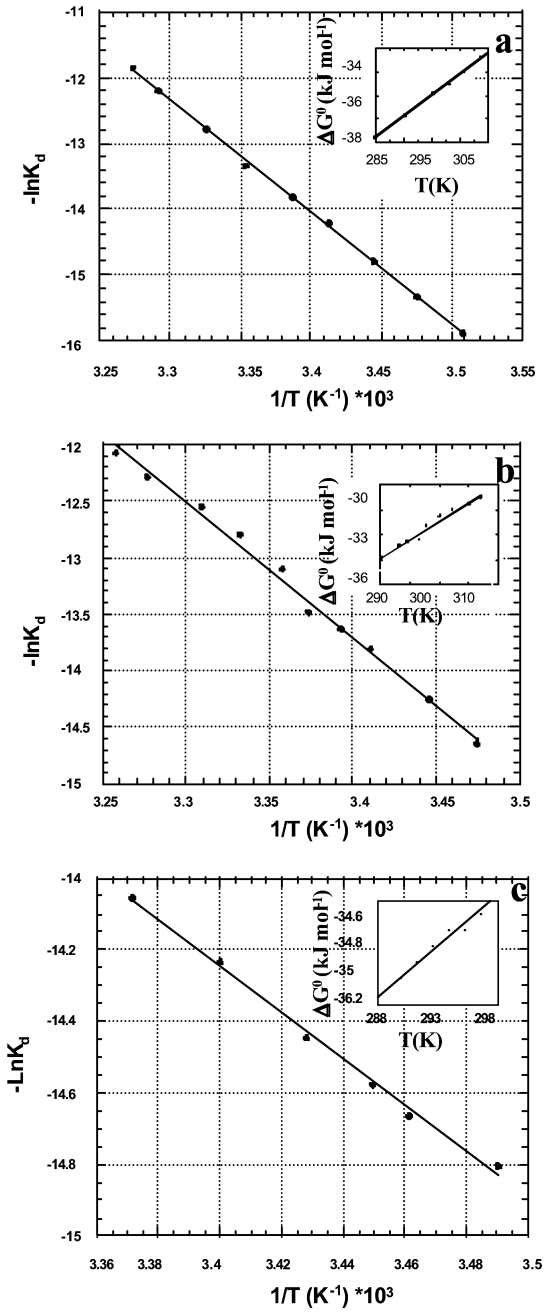

FIGURE 5: Determination of thermodynamic parameters $\Delta H°$ and $\Delta S°$ for B820 dissociation using the plot $-\ln K_d$ versus $1/T$: (a) nondigested, $t = 48$ h; (b) trypsin, $t = 48$ h; (c) GluC, $t = 2$ h. The amount of each species (B777 and B820) was calculated by decomposition of the absorption spectra recorded at different temperatures. The values calculated for $\Delta H°$ and $\Delta S°$ are -140, -99, and -28 kJ mol^{-1} and -0.22, -0.22, and -0.12 kJ mol^{-1} K^{-1} for nondigested, trypsin-treated B820, and GluC-treated B820. Variation of thermodynamic parameter $\Delta G°$ versus T is also shown.

by trypsin at position $R_{\alpha 3}$ results in a small, but significant, increase of the α-helix content of the B820 structure, suggesting that the first residues of the α polypeptide are in a random coil. Attack by GluC at position $E_{\beta 18}$ results in the loss of about 6 amino acids in the α-helical structure, while the 12 remaining ones must be either extended or in random coil in the B820. Remarkably, these results are exactly what could be expected using a modeled structure of the α and β polypeptides of LH1. The α and β polypeptides of the LH2 from *Rsp. molischianum* share close sequence homology with those of *Rsp. rubrum* (26% and 52% sequence identity, respectively). The structure of this LH2 was thus used as a matrix to build a *Rsp. rubrum* B820 structural model. The latter is little different from the *Rsp. molischianum* structure (rms deviation of 0.48 Å for the 94 Cα atoms) and was deposited on PDB with the PDB entry 1NWO. Twelve amino acids from the α polypeptide from *Rsp. rubrum* were however not included in this model, as they have no equivalent in *Rsp. molischianum* (Figures 1 and 6). In our model, the α helix starts at positions 10 and 14 on the α and β polypeptides, respectively. Taking into account both this structure and the sequence homologies between the LH1 from *Rsp. rubrum* and the LH2 from *Rsp. molischianum* (Figure 1), a small increase in the α-helical content is expected after the trypsin cleavage, while 6 residues in the α-helix (30%) should be deleted from the protein by the GluC cleavage at position $E_{\beta 18}$. This indicates that the conformation of the amino-terminal end of these polypeptides is likely to be similar and also that both protease attacks induce at best a very slight reorganization of the polypeptide backbone in the B820.

The variation of enthalpy accompanying the $\alpha\beta$ association drops down by at least 30% when the first three amino acids of the α polypeptide are cleaved by trypsin and more dramatically upon the removal of the amino-terminal part of the β polypeptide by the GluC protease. Pandit et al. proposed that at least half of the energy necessary to stabilize the B820 should arise from H-bonds formed on the carboxy terminus of the polypeptide and from the BChl/BChl interactions (*14*). Our results suggest that these interactions should not play an important role in the dimer stabilization but rather that the interactions involving the amino-terminal ends of the α and β polypeptides are dominant in their association process, in reasonable agreement with previous qualitative work performed by Meadows et al., which showed that it was in general more difficult to reconstitute B820 from protease-cleaved polypeptides (*19*). In the absence of a crystallographic structure, these authors proposed that this stabilization was due to electrostatic interactions (*19*). As early as 1994, Sturgis and Robert suggest that the largest part of the driving energy leading to the B820 subunit arises from hydrophobic interactions (*13*, *15*, *16*, *29*). The formation of the $\alpha\beta$ heterodimer is thus mainly driven by hydrophobic interactions occurring at the membrane interface. This conclusion is supported by the crystallographic structure of LH2 from *Rsp. molischianum*. In the latter, although direct contacts between the α and the β polypeptides are essentially located at the membrane interface, involving both their amino- and carboxy-terminal ends, little, if any, interaction of electrostatic nature can be observed. The situation is similar in the structural model of B820 (Figure 6).

It is of interest to analyze the hydrophobic contacts between the polypeptides to understand the structural features which are responsible for the stability of the heterodimer (in the following, the amino acid numbering used will refer to that of Figure 1, for both *Rsp. molischianum* and *Rsp. rubrum*). On the carboxy-terminal side, many contacts involve the BChl molecules, and side chain−side chain interactions mainly involve contacts between tryptophans $W_{\beta 44}$ and $W_{\alpha 40}$ and between the hydrophobic part of the lysine $R_{\beta 45}$ and both $F_{\alpha 38}$ and $W_{\beta 44}$. This important location for $R_{\beta 45}$ may explain why no cleavage is observed at the level of this residue in the presence of trypsin. On the amino-

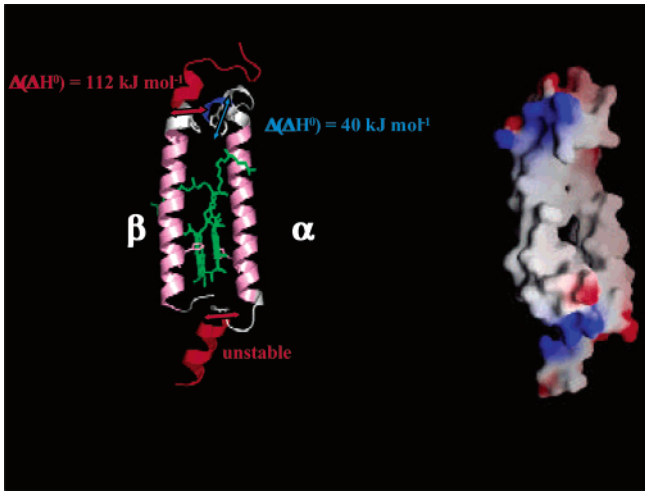

FIGURE 6: Structural modeling of B820. (a, left) Localization of cleavage sites on B820. The *Rsp. molischianum* LH2 (PDB entry 1LGH) structure was used as a matrix to construct the model. The Swiss-Model server (*24*) was used to generate the structure of LH1 in dimeric form. The Bchl were positioned using the 1LGH structure. The dimer and the complex were energy minimized in 100 steps with a dielectric constant of 1 using the program CNS (*25*). The backbone of each polypeptide is shown as a ribbon and the location of cleavage sites by arrows (blue for trypsin and red for GluC). (b, right) Electrostatic surface of the B820 dimer (without Bchl). The figure was produced by the GRASP software (*35*). The positively and negatively charged residues are indicated by the blue and red colors, respectively.

terminal side, the most striking structure is the position of $W_{\alpha 5}$ which lies at the interface between the polypeptides. It is involved in a number of hydrophobic interactions, with $I_{\alpha 4}$, $P_{\alpha 10}$, and $L_{\alpha 14}$ and with $L_{\beta 8}$, $A_{\beta 16}$, and $H_{\beta 20}$. The latter lies very close to this tryptophan (2.3 Å), at a distance actually short enough so that a H-bond could be formed between the NH groups of the indole ring and the imidazole ring, provided the deprotonated nitrogen atom of the latter faces the tryptophan side chain. This tryptophan thus constitutes the heart of a small hydrophobic cluster close to the membrane interface (a hydrophobic pocket). It is strictly conserved in the sequence of LH polypeptides, as well as $H_{\beta 20}$, and all of its partner amino acids are also either strictly conserved or replaced by very similar residues in other homologous LH proteins (*31*). The $H_{\beta 20}$ was for long thought to be the binding site of the 800 nm absorbing BChl in LH2, as it was strictly conserved in these complexes (*31*). It is worth noting that mutations of the amino acid equivalent to $H_{\beta 20}$ in LH2 from *Rhodobacter sphaeroides* have been reported to have a destabilizing effect on these complexes (*32*), in line with our present conclusions.

In native LH proteins, a carotenoid molecule is present, which ensures many hydrophobic contacts between the polypeptides of each dimeric subunit (*33*). In LH1 from wild-type *Rsp. rubrum*, each $\alpha\beta$ dimer binds a spirilloxanthin molecule, which is absent in the B820. In LH2, these molecules are essential for the in vivo assembly of the protein (*34*). Although LH1 may assemble without carotenoid, it is likely that the absence of these molecules induces defects in the molecular contacts between the LH polypeptides. Then, proper molecular contacts on the amino-terminal side between the α and β polypeptides may become essential for dimer formation. In other words, in native proteins, the role of the perimembrane extensions may become less essential than observed in this work for the association process, additional driving force being present because of the hydrophobic interactions engaged by the carotenoid molecules. However, they certainly play a role in the stability of these complexes.

CONCLUSION

In this paper, we show that the amino-terminal extensions of the polypeptides from LH1 from *Rsp. rubrum* play a dominant role in the dimerization process of these polypeptides, and we were able to quantify this role. Altogether, this constitutes the first attempt of such quantification for membrane protein interactions. An original molecular mechanism for the polypeptide/polypeptide association could be suggested, which consists of the presence of hydrophobic pockets at the membrane interface. Using the crystallographic structure of the LH2 from *Rsp. molischianum*, we attempted to determine which amino acids were likely to participate to this interaction, but their individual role still remains to be quantified by using sequence variants obtained by molecular biology techniques.

ACKNOWLEDGMENT

We are indebted to C. Mayer (Université Paris 6) and F. Rodier (CNRS, Gif/Yvette) for help in performing structural modeling and GRASP representation.

REFERENCES

1. Dawson, J. P., Weinger, J. S., and Engelman, D. M. (2002) Motifs of serine and threonine can drive association of transmembrane helices, *J. Mol. Biol. 316*, 799−805.
2. Senes, A., Ubarretxena-Belandia, I., and Engelman, D. M. (2001) The Cα- - -H···O hydrogen bond: a determinant of stability and specificity in transmembrane helix interactions, *Proc. Natl. Acad. Sci. U.S.A. 98*, 9056−9061.
3. Ubarretxena-Belandia, I., and Engelman, D. M. (2001) Helical membrane proteins: diversity of functions in the context of simple architecture, *Curr. Opin. Struct. Biol. 11*, 370−376.
4. Scheuring, S., Seguin, J., Marco, S., Levy, D., Robert, B., and Rigaud, J. L. (2003) Nanodissection and high-resolution imaging of the *Rhodopseudomonas viridis* photosynthetic core complex in native membranes by AFM. Atomic force microscopy, *Proc. Natl. Acad. Sci. U.S.A. 100*, 1690−1693.
5. Karrasch, S., Bullough, P. A., and Ghosh, R. (1995) The 8.5 Å projection map of the light-harvesting complex I from Rhodospirillum rubrum reveals a ring composed of 16 subunits, *EMBO J. 14*, 631−638.
6. Walz, T., and Ghosh, R. (1997) Two-dimensional crystallization of the light-harvesting I-reaction center photounit from *Rhodospirillum rubrum*, *J. Mol. Biol. 265*, 107−111.
7. Walz, T., Jamieson, S. J., Bowers, C. M., Bullough, P. A., and Hunter, C. N. (1998) Projection structures of three photosynthetic complexes from *Rhodobacter sphaeroides*: LH2 at 6 Å, LH1 and RC-LH1 at 25 Å, *J. Mol. Biol. 282*, 833−845.
8. Jamieson, S. J., Wang, P., Qian, P., Kirkland, J. Y., Conroy, M. J., Hunter, C. N., and Bullough, P. A. (2002) Projection structure of the photosynthetic reaction centre-antenna complex of *Rhodospirillum rubrum* at 8.5 Å resolution, *EMBO J. 21*, 3927−3935.
9. Van Grondelle, R. (1985) Excitation energy transfer, trapping and annihilation in photosynthetic systems, *Biochim. Biophys. Acta 811*, 147−195.
10. Westerhuis, W. H. J., Hunter, C. N., Van Grondelle, R., and Niederman, R. A. (1999) Modeling of Oligomeric-State Dependent Spectral Heterogeneity in the B875 Light-Harvesting Complex of *Rhodobacter sphaeroides* by Numerical Simulation, *J. Phys. Chem. B 103*, 7733−7742.
11. Loach, P. A., and Parkes-Loach, P. S. (1995) Structure−function relationships in core light-harvesting complexes (LHI) as determined by characterization of the structural subunit and by reconstitution experiments, in *Anoxygenic Photosynthetic Bacteria*

(Blankenship, R. E., Madigan, M. T., and Bauer, C. E., Eds.) pp 437−471, Kluwer Academic, Dordrecht.
12. Sturgis, J. N., and Robert, B. (1997) Pigment binding-site and electronic properties in light-harvesting proteins of purple bacteria, *J. Phys. Chem. B 101*, 7227−7231.
13. Sturgis, J. N., and Robert, B. (1994) Thermodynamics of membrane polypeptide oligomerization in light-harvesting complexes and associated structural changes, *J. Mol. Biol. 238*, 445−454.
14. Pandit, A., Visschers, R. W., van Stokkum, I. H., Kraayenhof, R., and van Grondelle, R. (2001) Oligomerization of light-harvesting I antenna peptides of *Rhodospirillum rubrum*, *Biochemistry 40*, 12913−12924.
15. Arluison, V., Seguin, J., and Robert, B. (2002) Reaction order and nature of reactants during oligomers dissociation of light-harvesting complex I from *Rsp. rubrum* G9+, *FEBS Lett. 516*, 40−42.
16. Arluison, V., Seguin, J., and Robert, B. (2002) Biochemical characterization of the dissociated forms from the core antenna proteins from purple bacteria, *Biochemistry 41*, 11812−11819.
17. Parkes-Loach, P. S., Sprinkle, J. R., and Loach, P. A. (1988) Reconstitution of the B873 light-harvesting complex of *Rhodospirillum rubrum* from the separately isolated α- and *β*-polypeptides and bacteriochlorophyll a, *Biochemistry 27*, 2718−2727.
18. Ghosh, R., Hauser, H., and Bachofen, R. (1988) Reversible dissociation of the B873 light-harvesting complex from *Rhodospirillum rubrum* G9+, *Biochemistry 27*, 1004−1014.
19. Meadows, K. A., Parkes-Loach, P. S., Kehoe, J. W., and Loach, P. A. (1998) Reconstitution of core light-harvesting complexes of photosynthetic bacteria using chemically synthesized polypeptides. 1. Minimal requirements for subunit formation, *Biochemistry 37*, 3411−3417.
20. Kehoe, J. W., Meadows, K. A., Parkes-Loach, P. S., and Loach, P. A. (1998) Reconstitution of core light-harvesting complexes of photosynthetic bacteria using chemically synthesized polypeptides. 2. Determination of structural features that stabilize complex formation and their implications for the structure of the subunit complex, *Biochemistry 37*, 3418−3428.
21. Koepke, J., Hu, X., Muenke, C., Schulten, K., and Michel, H. (1996) The crystal structure of the light-harvesting complex II (B800−850) from *Rhodospirillum molischianum*, *Structure 4*, 581−597.
22. Brunisholz, R. A., Wiemken, V., Suter, F., Bachofen, R., and Zuber, H. (1984) The light-harvesting polypeptides of *Rhodospirillum rubrum*. II. Localization of the amino-terminal regions of the light-harvesting polypeptides B 870-α and B 870-*β* and the reaction-center subunit L at the cytoplasmic side of the photosynthetic membrane of *Rhodospirillum rubrum* G-9, *Hoppe-Seyler's Z. Physiol. Chem. 365*, 689−701.
23. Chang, M. C., Callahan, P. M., Parkes-Loach, P. S., Cotton, T. M., and Loach, P. A. (1990) Spectroscopic characterization of the light-harvesting complex of *Rhodospirillum rubrum* and its structural subunit, *Biochemistry 29*, 421−429.
24. Guex, N., and Peitsch, M. C. (1997) SWISS-MODEL and the Swiss-PdbViewer: an environment for comparative protein modeling, *Electrophoresis 18*, 2714−2723.
25. Brunger, A. T., Adams, P. D., Clore, G. M., DeLano, W. L., Gros, P., Grosse-Kunstleve, R. W., Jiang, J. S., Kuszewski, J., Nilges, M., Pannu, N. S., Read, R. J., Rice, L. M., Simonson, T., and Warren, G. L. (1998) Crystallography & NMR system: A new software suite for macromolecular structure determination, *Acta Crystallogr., D: Biol. Crystallogr. 54*, 905−921.
26. Vegh, A. P., and Robert, B. (2002) Spectroscopic characterisation of a tetrameric subunit form of the core antenna protein from *Rhodospirillum rubrum*, *FEBS Lett. 528*, 222−226.
27. Olsen, J. D., Sockalingum, G. D., Robert, B., and Hunter, C. N. (1994) Modification of a hydrogen bond to a bacteriochlorophyll a molecule in the light-harvesting 1 antenna of *Rhodobacter sphaeroides*, *Proc. Natl. Acad. Sci. U.S.A. 91*, 7124−7128.
28. Sturgis, J. N., Olsen, J. D., Robert, B., and Hunter, C. N. (1997) Functions of conserved tryptophan residues of the core light-harvesting complex of *Rhodobacter sphaeroides*, *Biochemistry 36*, 2772−2778.
29. Pandit, A., Ma, H., Van Stokkum, I. H., Gruebele, M., and Van Grondelle, R. (2002) Time-resolved dissociation of the light-harvesting 1 complex of *Rhodospirillum rubrum*, studied by infrared laser temperature jump, *Biochemistry 41*, 15115−15120.
30. Paternostre, M., Viard, M., Meyer, O., Ghanam, M., Ollivon, M., and Blumenthal, R. (1997) Solubilization and reconstitution of vesicular stomatitis virus envelope using octylglucoside, *Biophys. J. 72*, 1683−1694.
31. Zuber, H., and Cogdell, R. J. (1995) Structure and organization of purple bacterial antenna complexes, *Adv. Photosynth. 2*, 315−348.
32. Crielaard, W., Visschers, R. W., Fowler, G. J. S., van Grondelle, R., Hellingwerf, K. J., and Hunter, C. N. (1994) Probing the B800 bacteriochlorophyll binding site of the accessory light-harvesting complex from *Rhodobacter sphaeroides* using site-directed mutants. I. Mutagenegenesis, effects on binding, function and electronic behaviour of its carotenoids, *Biochim. Biophys. Acta 1183*, 473−482.
33. McDermott, G., Prince, S. M., Freer, A. A., Hawthornthwaite-Lawless, A. M., Papiz, M. Z., Cogdell, R. J., and Isaacs, N. W. (1995) Crystal structure of an integral membrane light-harvesting complex from photosynthetic bacteria, *Nature 374*, 517−521.
34. Lang, H. P., and Hunter, C. N. (1994) The relationship between carotenoid biosynthesis and the assembly of the light-harvesting LH2 complex in *Rhodobacter sphaeroides*, *Biochem. J. 298*, 197−205.
35. Nicholls, A., Sharp, K. A., and Honig, B. (1991) Protein folding and association: insights from the interfacial and thermodynamic properties of hydrocarbons, *Proteins 11*, 281−296.
36. Zuber, H. (1990) Considerations on the structural principles of the antenna complexes of phototrophic bacteria, in *Molecular Biology of Membrane Bound Complexes in Phototrophic Bacteria* (Drews, G., and Dawes, E. A., Eds.) pp 161−180, Plenum Press, New York.
37. Germeroth, L., Lottspeich, F., Robert, B., and Michel, H. (1993) Unexpected similarity of the B 800−850 light-harvesting complex of *Rhodospirillum molichianum* with the light-harvesting complex I of other purple bacteria, *Biochemistry 32*, 5615−5621.

BI030205V